Homoleptic Perchlorophenyl "Ate" Complexes of Thorium(IV) and Uranium(IV)

Osvaldo Ordoñez,[a] Xiaojuan Yu,[b] Guang Wu,[a] Jochen Autschbach,*[,b] and Trevor W. Hayton*[,a]

a. Department of Chemistry and Biochemistry, University of California Santa Barbara, Santa Barbara, CA 93106

b. Department of Chemistry, University at Buffalo, State University of New York, Buffalo, NY 14260

*To whom correspondence should be addressed. Email: jochena@buffalo.edu, hayton@chem.ucsb.edu

Abstract

Reaction of $AnCl_4(DME)_n$ (An = Th, n = 2; U, n = 0) with 5 equiv of LiC_6Cl_5 in Et_2O resulted in the formation of homoleptic actinide-aryl "ate" complexes $[Li(DME)_2(Et_2O)]_2[Li(DME)_2][Th(C_6Cl_5)_5]_3$ ([Li][**1**]) and $[Li(Et_2O)_4][U(C_6Cl_5)_5]$ ([Li][**2**]). Similarly, reaction of $AnCl_4(DME)_n$ (An = Th, n = 2; U, n = 0) with 3 equiv of LiC_6Cl_5 in Et_2O resulted in formation of heteroleptic actinide-aryl "ate" complexes $[Li(DME)_2(Et_2O)][Li(Et_2O)_2][ThCl_3(C_6Cl_5)_3]$ ([Li][**3**]) and $[Li(Et_2O)_3][UCl_2(C_6Cl_5)_3]$ ([Li][**4**]). Density functional calculations show that the An-C_{ipso} σ-bonds are considerably more covalent for the uranium complexes vs. the thorium analogues, in line with past results. Additionally, good agreement between experiment and calculations is obtained for the $^{13}C_{ipso}$ NMR chemical shifts in [Li][**1**] and [Li][**3**]. The calculations demonstrate a deshielding by ca. 29 ppm from spin-orbit coupling effects originating at Th, which is a direct consequence of 5f orbital participation in the Th-C bonds.

Introduction

Homoleptic actinide alkyl complexes have proven to be excellent testbeds for the study of electronic structure and bonding within these enigmatic elements.[1–3] As a result, a number of homoleptic actinide alkyl complexes have been synthesized in the last 10 years.[4–18] These complexes include $[Li(DME)_n][An(CH_2SiMe_3)_5]$ (An = Th, n = 2; An = U, n = 3),[8,10] reported by us, $[Li(THF)_4][Li(THF)_2][UMe_6]$,[4] reported by Neidig and co-workers, and $[U(CH_2Ph)_4]$,[7] reported by Bart and co-workers. In contrast, homoleptic actinide aryl complexes remain exceedingly rare, in part because of their tendency to undergo facile *ortho* C-H bond activation.[19–21] For example, the first structurally characterized homoleptic uranium aryl, $[U(C_6H_3\text{-}2,6\text{-}(C_6H_4\text{-}4\text{-}^tBu)_2)_3]$, was only isolated in 2016 by Arnold and co-workers. Its isolation required the use of 4-^{t}BuC_6H_4 *ortho* substituents on the aryl ligand to prevent *ortho* C-H bond activation.[20] Even with the 4-^{t}BuC_6H_4 substituents, however, $[U(C_6H_3\text{-}2,6\text{-}(C_6H_4\text{-}4\text{-}^tBu)_2)_3]$ still decomposes on standing at room temperature, specifically by activation of an *ortho* C-H bond located on the 4-^{t}BuC_6H_4 substituent. Additionally, we and others have used "ate" complex formation to generate homoleptic An(IV) aryl complexes, including $[Li(DME)_3]_2[Th(C_6H_5)_6]$[19] and $[Li(THF)_4][(THF)LiU(C_6H_5)_6]$.[22] These complexes are stabilized by saturation of the actinide coordination sphere, which presumably disfavors the *ortho* C-H bond activation reaction.[19] Nonetheless, $[Li(THF)_4][(THF)LiU(C_6H_5)_6]$ is still exceptionally thermally sensitive, and could only be isolated at -80 °C.[22] The use of pendant donor groups can also stabilize An-C_{aryl} bonds, as was observed for $[Th(\eta^2\text{-}N,C\text{-}C_6H_4\text{-}o\text{-}CH_2NMe_2)_4]$,[21] $[Cp^*_2U(\eta^2\text{-}N,C\text{-}(o\text{-}C_6H_4)NPh)]$,[23] and $[Cp^*_2U(\eta^2\text{-}Te,C\text{-}(o\text{-}C_6H_4)Te)]$.[24]

Many of these actinide aryl complexes are attractive targets for studying covalency via ^{13}C NMR spectroscopy. NMR spectroscopy has been previously used as a tool to evaluate covalency

in An-L and Ln-L bonding.[19,25–33] In the case of actinide aryl complexes, the ^{13}C NMR chemical shifts for the C_{ipso} environments are strongly affected by spin-orbit (SO) coupling, a consequence of 5f (and to a lesser extent, 6d) orbital participation in the An-C σ-bond.[25] In particular, in $5f^0$ systems with low-lying, empty 5f or 6d orbitals, SO coupling tends to cause ^{13}C deshielding as long as the An-C σ-bond has sizable C 2s character.[34] For example, the ^{13}C NMR spectrum of $[Li(DME)_3]_2[Th(C_6H_5)_6]$ features a C_{ipso} chemical shift of 220.5 ppm, with a calculated 44 ppm downfield contribution from SO coupling.[19] This SO deshielding correlates to the 5f (and 6d) participation in the Th-C bond. In the case of $[Th(C_6H_5)_6]^{2-}$, specifically, the Th-C bonds were calculated to have 15% weight each from Th atomic orbitals (AOs), of which 71/15% was from 6d/5f participation, respectively.

We recently reported the syntheses of the first structurally characterized uranyl(VI) aryl complexes, $[Li(Et_2O)_2(THF)][UO_2(C_6Cl_5)_3]$ and $[Li(THF)_4][UO_2(C_6Cl_5)_3(THF)]$, via reaction of $[UO_2Cl_2(THF)_2]$ with 3 equiv of LiC_6Cl_5. These complexes feature surprisingly good thermal stability,[25] which we ascribed, in part, to the *ortho*-Cl substitution of the $[C_6Cl_5]^-$ ligand. Given this precedent, we rationalized that the $[C_6Cl_5]^-$ ligand could also stabilize homoleptic U(IV) and Th(IV) complexes. Additional support for this hypothesis comes from large number of homoleptic transition metal perhalophenyl complexes that have been reported over the past 25 years.[35–44] Despite these past synthetic achievements, however, no homoleptic perhalophenyl complexes are known for actinides. Additionally, the only heteroleptic perhalophenyl actinide complexes are the aforementioned uranyl(VI) species,[25] making this a potentially fruitful avenue of investigation. Herein, we describe the synthesis and characterization of two homoleptic actinide-aryl "ate" complexes $[Li(DME)_2(Et_2O)]_2[Li(DME)_2][Th(C_6Cl_5)_5]_3$ ([Li][**1**]) and $[Li(Et_2O)_4][U(C_6Cl_5)_5]$ ([Li][**2**]). During the course of these investigations, we also isolated the closely related heteroleptic

actinide-aryl "ate" complexes, $[Li(DME)_2(Et_2O)][Li(Et_2O)_2][ThCl_3(C_6Cl_5)_3]$ ([Li][**3**]) and $[Li(Et_2O)_3][UCl_2(C_6Cl_5)_3]$ ([Li][**4**]). The electronic structures of all four complexes were analyzed using relativistic density functional theory (DFT) calculations, with the aim of quantifying the 5f subshell participation in the An-C_{ipso} bonds.

Results and Discussion

Addition of cold (-25 °C) solutions of 5 equiv of LiC_6Cl_5[45] to cold (-25 °C) suspensions of $AnCl_4(DME)_n$ (An = Th, n = 2; U, n = 0) in Et_2O results in immediate formation of orange solutions, concomitant with the deposition of flocculent brown-orange precipitates. Work-up of the thorium reaction mixture, followed by crystallization from dichloromethane, affords $[Li(DME)_2(Et_2O)]_2[Li(DME)_2][Th(C_6Cl_5)_5]_3$ ([Li][**1**]), which can be isolated as colorless plates in 20% yield (Scheme 1). Work-up of the uranium reaction mixture, followed by crystallization from Et_2O, affords $[Li(Et_2O)_4][U(C_6Cl_5)_5]$ ([Li][**2**]), which can be isolated as yellow plates in 57% yield (Scheme 1). Interestingly, we see no evidence for the formation of octahedral $[An(C_6Cl_5)_6]^{2-}$-type complexes, even when 6 equiv of $Li(C_6Cl_5)$ are used in the reaction.

Scheme 1.

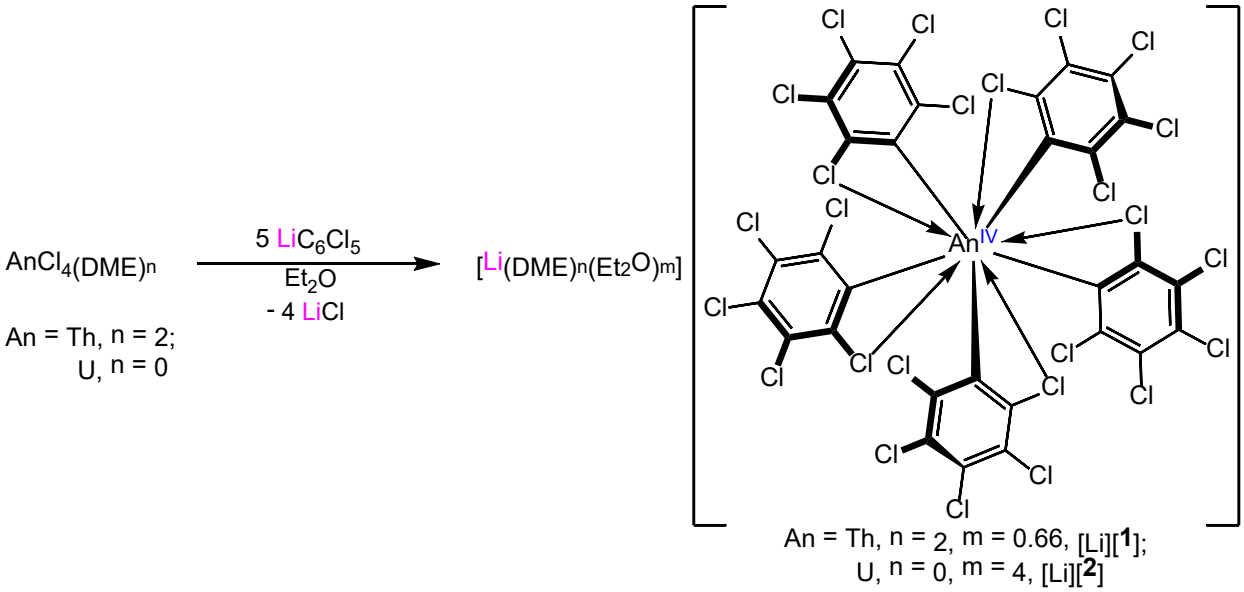

Curiously, the reaction of $ThCl_4(DME)_2$ with 4 equiv of LiC_6Cl_5, performed in an attempt to make the neutral perchlorophenyl complex, $[Th(C_6Cl_5)_4]$, resulted in isolation of heteroleptic Th aryl complex, $[Li(DME)_2(Et_2O)][Li(Et_2O)_2][ThCl_3(C_6Cl_5)_3]$ ([Li][**3**]), in low yield, according to an X-ray crystallographic analysis of the crystals isolated upon work-up. Complex [Li][**3**] can be made rationally by addition of 3 equiv of LiC_6Cl_5 to a cold (-25 °C) suspension $ThCl_4(DME)_2$ in Et_2O. When synthesized using this stoichiometry, [Li][**3**] can be isolated as colorless plates in 54% yield (Scheme 2). Similarly, addition of 3 equiv of LiC_6Cl_5 to a cold (-25 °C) suspension UCl_4 in Et_2O results in formation of $[Li(Et_2O)_3][UCl_2(C_6Cl_5)_3]$ ([Li][**4**]), which can be isolated as amber plates in 40% yield after work-up (Scheme 2). The reactions of UCl_4 with 4 equiv of LiC_6Cl_5 also results in formation of [Li][**4**], in similar yields to the 3 equiv reaction.

Scheme 2.

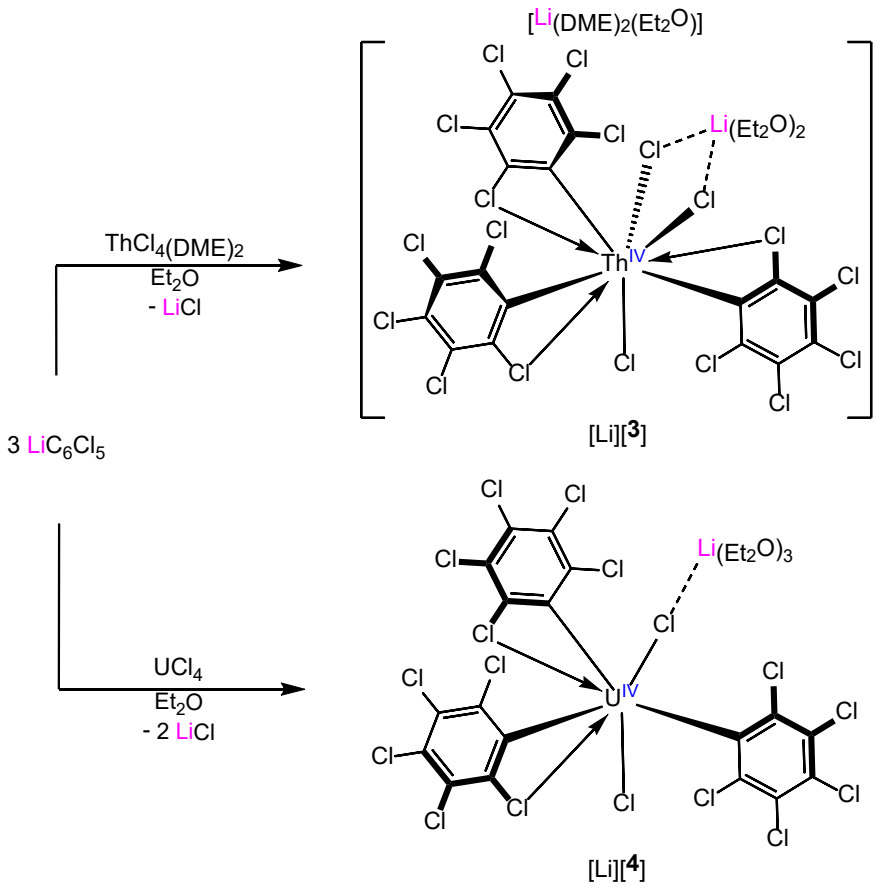

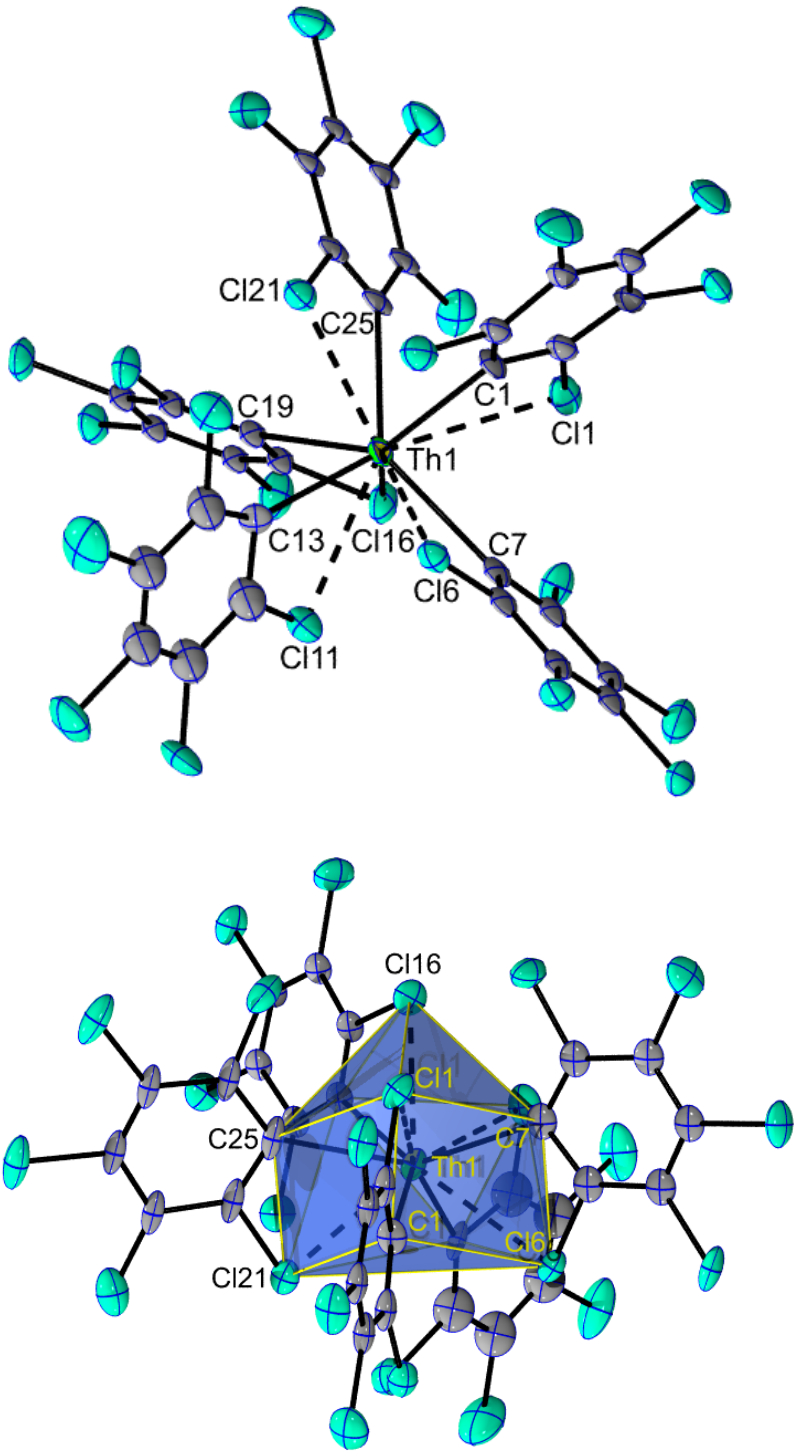

Figure 1. Solid-state molecular structure of [Li][**1**]·2.5Et_2O·2CH_2Cl_2 shown with 50% probability ellipsoids (top). Solid-state molecular structure of [Li][**1**]·2.5Et_2O·2CH_2Cl_2 with the sphenocorona

polygon shown in blue (bottom). All hydrogen atoms, solvate molecules, two $[Th(C_6Cl_5)_5]^-$ moieties, and Li^+ counterions have been omitted for clarity.

Both [Li][**1**] and [Li][**2**] are air- and moisture-sensitive crystalline solids that are soluble in ethereal solvents, methylene chloride, and benzene, and slightly soluble in hexanes. Additionally, [Li][**1**] is soluble in pyridine and acetonitrile, however [Li][**2**] reacts immediately upon dissolution in pyridine, resulting in formation of an intractable dark brown solution. Similarly, dissolution of [Li][**2**] in acetonitrile results in immediate formation of an intractable orange-brown solution concomitant with precipitation of a dark brown solid. Both [Li][**1**] and [Li][**2**] exhibit moderate thermal stability in solution. For example, solutions of [Li][**1**] or [Li][**2**] in CH_2Cl_2 exhibit minimal evidence of decomposition after standing at room temperature for 1 h. However, on standing at room temperature for 24 h, solutions of [Li][**1**] in methylene chloride-d_2 exhibit partial conversion to [Li][**3**], according to $^{13}C\{^1H\}$ NMR spectroscopy (Figure S4), presumably via C-Cl bond activation of the solvent. In contrast, solutions of [Li][**2**] completely convert into intractable mixtures in methylene chloride-d_2 over this time frame (Figure S6). It is not immediately apparent why [Li][**2**] is more reactive that [Li][**1**], but we note that a similar reactivity pattern is observed for $[An(C_6H_5)_6]^{2-}$ and $[Cp^*_2An(C_6H_5)_2]$ (An = Th, U),[19,22,46] where the uranium analogues exhibit greater thermal sensitivity than the thorium analogues.

Complex [Li][**1**] crystallizes in the monoclinic space group $P2_1/n$ with three independent molecules in the asymmetric unit (Figure 1 and Table 1). It crystallizes as the Et_2O and CH_2Cl_2 solvate, [Li][**1**]·2.5Et_2O·2CH_2Cl_2. Its asymmetric unit reveals one ten-coordinate thorium center and two nine-coordinate thorium centers. According to the continuous shape measure,[47] the 10-coordinate Th center, Th1, is best described as a C_{2v}-symmetric sphenocorona, wherein the two square faces are defined by C1, C7, Cl1, and Cl16, and C1, C25, Cl1, and Cl21, respectively. This

geometry is common for 10-coordinate complexes featuring bidentate ligands.[48] The two 9-coordinate metal centers are best described as distorted tricapped trigonal prisms.[49,50] For Th2, the three capping atoms are C31, C43, and Cl46, whereas for Th3, the three capping atoms are C73, C85, and Cl51. The ten coordinate center in [Li][**1**] features five Th-C σ-bonds and five Cl→Th dative interactions involving the *ortho*-Cl atoms of the C_6Cl_5 ligands, although one of these Cl→Th dative interactions is quite long (Th1-Cl1 = 3.257(5) Å; see below for more discussion). The nine coordinate centers in [Li][**1**] are formed by five An-C σ-bonds and four Cl→An dative interactions. The κ^2 coordination mode generated by the Cl→An dative interaction has been previously observed for a handful of $[C_6Cl_5]^-$ complexes, including $Pt(C_6Cl_5)_4$.[38,42,43] The average Th-C bond length in [Li][**1**] is 2.65 Å (range = 2.628(18) – 2.693(18) Å), which is similar those found in other σ-bonded thorium aryl complexes.[19,21] For example, the Th-C bond length in $[Li(DME)_3]_2[Th(C_6H_5)_6]$[19] is 2.589(3) Å, whereas the average Th-C bond length in $[Th(2\text{-}C_6H_4CH_2NMe_2)_4]$[21] is 2.549(2) Å (range = 2.497(3) – 2.544(3) Å). Additionally, both the 10-coordinate and 9-coordinate Th centers in [Li][**1**] exhibit identical average Th-C bond lengths. The aryl rings in [Li][**1**] feature disparate Th-C_{ipso}-C_{ortho} angles, a consequence of the Cl→An dative interactions. For example, the Th-C1-C2 angle is 110(1)°, whereas the Th1-C1-C6 angle is 134(1)°. The average Cl→Th bond length in [Li][**1**] is 3.09 Å (range = 3.018(5) – 3.257(5) Å). No other complexes with Cl→An interactions are available for comparison, but several complexes with F→An interactions are known.[51] For example, the F→U distances in $[Cp^*_2Co][U(OB(C_6F_5)_3)_2(^{Ar}acnac)(OEt_2)]$[52] are 2.762(6) and 2.789(5) Å, whereas the F→U distances in $[U(N(C_6F_5)_2)_4]$ are 2.6480(11) and 2.5989(11) Å.[53] Not surprisingly, these values are much shorter than the Cl→An interactions observed in [Li][**1**]. One ten-coordinate and one nine-coordinate center in [Li][**1**] each exhibit an outer sphere cation $[Li(DME)_2(Et_2O)]^+$, while the other

nine-coordinate thorium center in [Li][**1**] features a $[Li(DME)_2]^+$ cation that also interacts with the *ortho*-Cl and *meta*-Cl atoms of one C_6Cl_5 ligand. The observation of two different Th coordination geometries in the solid-state can be explained by small differences in local crystal packing, and indicates that the long Cl→Th dative interaction (e.g., Th1-Cl1) is not particularly strong.

Complex [Li][**2**] crystallizes in the monoclinic space group $P2_1/c$ (Figure S15). The solid-state molecular structure of [Li][**2**] reveals a ten-coordinate uranium center formed by five An-C σ-bonds and five Cl→An dative interactions involving the *ortho*-Cl atoms of the C_6Cl_5 ligands.[48] According to the continuous shape measure,[47] the coordination geometry about the U center is best described as a C_{2v}-symmetric sphenocorona, wherein the two square faces are defined by Cl16, C13, Cl6, and Cl1, and C13, C25, Cl11, Cl16, respectively. The average U-C bond length in [Li][**2**] is 2.55 Å (range = 2.52(2) – 2.59(2) Å), which is shorter than the Th-C distances in [Li][**1**], consistent with smaller ionic radius of the U(IV) ion.[54] The U-C bond lengths in [Li][**2**] are also similar to those observed in other uranium aryl complexes, such as $[Li(Et_2O)_2(THF)][UO_2(C_6Cl_5)_3]$,[25] which features U-C distances from 2.55(1) to 2.63(1) Å, and $[Li(THF)_4][Li(THF)][U(C_6H_5)_6]$,[22] which features an average U-C bond length of 2.52 Å. The latter structure also features H→U agostic interactions, which are similar to the Cl→An interactions found in [Li][**1**] and [Li][**2**]. The aryl rings in [Li][**2**] feature disparate U-C_{ipso}-C_{ortho} angles (e.g., U1-C1-C2 = 113(1)°, U1-C1-C6 = 135(1)°), which is a consequence of the Cl→An dative interactions. Finally, the average Cl→U distance in [Li][**2**] is 3.13 Å (range = 3.006(4) – 3.250(4) Å), which is similar to that found in [Li][**1**].

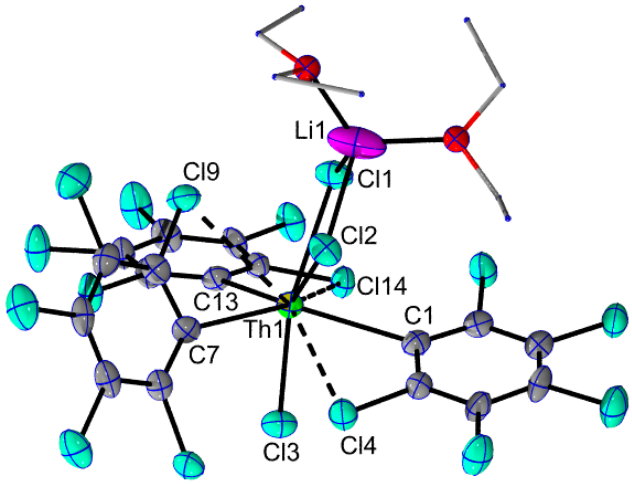

Figure 2. Solid-state molecular structure of [Li][**3**] shown with 50% probability ellipsoids. All hydrogen atoms and a $[Li(DME)_2(Et_2O)]^+$ counterion have been omitted for clarity.

Complex [Li][**3**] crystallizes in the triclinic space group *P*1 (Figure 2). Its solid-state molecular structure reveals a 9-coordinate thorium center bound by three chloride ligands, three carbon atoms of the pentachlorophenyl ligands, and three Cl→Th dative interactions involving the *ortho*-Cl atoms of the pentachlorophenyl ligands. The coordination geometry about its Th center can be described as distorted tricapped trigonal prism,[55] wherein the three capping atoms are Cl4, Cl9, and Cl14. The average Th-C bond length in [Li][**3**] is 2.65 Å (range = 2.631(6) – 2.654(6) Å), which is similar to Th-C bond lengths in [Li][**1**]. The average Th-Cl distance in [Li][**3**] is 2.77 Å (range = 2.671(2) – 2.839(2) Å), which is slightly longer than the average Th-Cl bond length in $ThCl_4(DME)_2$ (2.690 Å),[56] whereas the average Cl→An dative interactions in [Li][**3**] is 3.19 Å (range = 3.148(2) – 3.248(2) Å). Finally, the $[Li(Et_2O)_2]^+$ cation in [Li][**3**] features bridging interaction with two chloride ligands. The resulting Li-Cl distances are 2.37(2) Å and 2.39(2) Å.

Complex [Li][**4**] also crystallizes in the triclinic space group *P*1 (Figure 3). Its solid-state molecular structure reveals a 7-coordinate uranium center bound by two chloride ligands, three carbon atoms of the pentachlorophenyl ligand, and two long Cl→U dative interactions involving the *ortho*-Cl atoms of the pentachlorophenyl ligands (e.g., U1-Cl3 = 3.226(4), U1-Cl8 = 3.227(3) Å). Ignoring the long Cl→U dative interactions, the coordination geometry about the U center is best described as trigonal bipyramid. The average U-C bond length in [Li][**4**] is 2.50 Å (range = 2.50(1) – 2.51(1) Å) and is similar to that seen in [Li][**2**] but shorter than that seen in [Li][**3**], consistent with smaller ionic radius of U(IV) ion.[54] The average U-Cl bond length in [Li][**4**] is 2.59 Å (range = 2.591(4) – 2.594(4) Å), consistent with the average U-Cl bond length of 2.62 Å in $UCl_4(DME)_2$.[57] Finally, the $[Li(Et_2O)_3]^+$ cation in [Li][**4**] features a bridging interaction with a chloride ligand. The resulting Li-Cl distance is 2.69(5) Å.

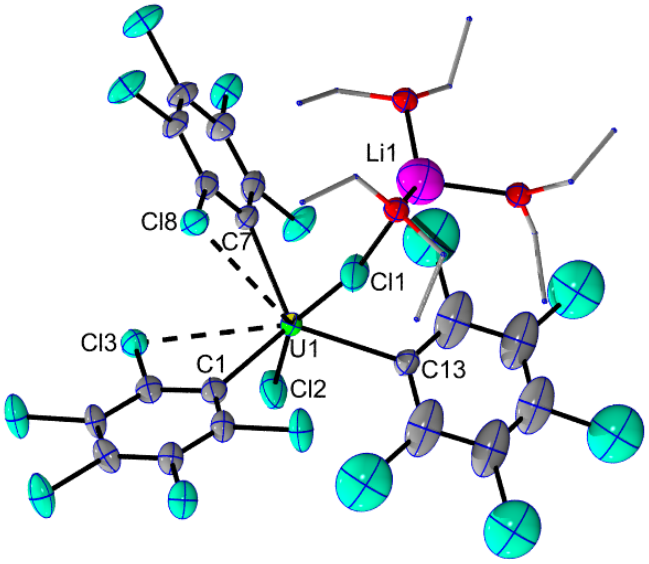

Figure 3. Solid-state molecular structure of [Li][**4**] shown with 50% probability ellipsoids. All hydrogen atoms have been omitted for clarity.

Table 1. Selected metrical parameters for [Li][**1**]·2.5Et_2O·2CH_2Cl_2, [Li][**2**], [Li][**3**], and [Li][**4**].

Complex	[Li][**1**]·2.5Et_2O·2CH_2Cl_2			[Li][**2**]	[Li][**3**]	[Li][**4**]
An-C	Th1	Th2	Th3	2.518(17) 2.537(15) 2.541(12) 2.555(17) 2.592(16)	2.631(6) 2.653(6) 2.654(6)	2.497(13) 2.504(13) 2.505(14)
	2.633(16) 2.646(17) 2.649(18) 2.670(19) 2.673(17)	2.628(18) 2.637(17) 2.639(16) 2.656(19) 2.678(19)	2.631(18) 2.641(18) 2.645(17) 2.66(2) 2.693(18)			
Cl→An	3.018(5) 3.068(5) 3.073(5) 3.101(4) 3.257(5)	3.033(5) 3.064(5) 3.069(4) 3.107(5)	3.073(5) 3.092(6) 3.115(5) 3.122(5)	3.006(4) 3.071(5) 3.121(4) 3.197(4) 3.255(4)	3.1489(19) 3.1776(17) 3.2477(17)	3.226(4) 3.227(3)
An-Cl					2.6702(17) 2.7887(18) 2.8390(18)	2.591(4) 2.594(4)

The $^{13}C\{^1H\}$ NMR spectrum of [Li][**1**], recorded at room temperature in dichloromethane-d_2, features a resonance at 198.78 ppm (Figure S2), attributable to the *ipso* carbon of the pentachlorophenyl ligand, as well as resonances at 138.66, 131.03, and 130.13 ppm, assignable to the *ortho*, *meta*, and *para* resonances of the pentachlorophenyl ligand, respectively. The $^{13}C\{^1H\}$ NMR spectrum of [Li][**3**], recorded at room temperature in dichloromethane-d_2, features a resonance at 201.01 ppm (Figure S9), attributable to the *ipso* carbon of the pentachlorophenyl ligand, as well as resonances at 137.20, 131.96, and 129.53 ppm, assignable to the *ortho*, *meta*, and *para* resonances of the pentachlorophenyl ligand, respectively. The observation of only one aryl environment for both [Li][**1**] and [Li][**3**] in their $^{13}C\{^1H\}$ NMR spectra is evidence for exchange of the Cl→Th dative interactions at a rate faster than the NMR time scale, which

renders the aryl ligands magnetically equivalent. The $^{13}C\{^1H\}$ NMR spectra of both [Li][**1**] and [Li][**3**] feature smaller downfield C_{ipso} resonances compared to $[Li(Et_2O)_2(THF)][UO_2(C_6Cl_5)_3]$, which featured a C_{ipso} resonance at 236.7 ppm.[25]

The $^7Li\{^1H\}$ NMR spectra for [Li][**1**] and [Li][**3**] in dichloromethane-d_2 feature sharp resonances at -0.79 ppm and -0.83 ppm, respectively (Figures S1 and S8). In contrast, the $^7Li\{^1H\}$ NMR spectrum of [Li][**2**] in dichloromethane-d_2 features a broad resonance at 0.52 ppm (Figure S5), consistent with the paramagnetism of this material. The $^7Li\{^1H\}$ NMR spectrum of [Li][**4**] in benzene-d_6 features a broad resonance at 29.59 ppm (Figure S11). The large downfield shift is consistent with formation of a contact ion pair in solution. Similar behavior has been observed previously for uranium aryl and uranium benzyne complexes.[58]

To gain a detailed understanding of the electronic structures and bonding interactions within [Li][**1**], [Li][**2**], [Li][**3**], and [Li][**4**], relativistic DFT calculations were performed on their anionic components, namely, $[\mathbf{1}]^-$, $[\mathbf{2}]^-$, $[\mathbf{3}]^-$, and $[\mathbf{4}]^-$.[59–61] Full computational details are described in the Supporting Information. The ground states of $[\mathbf{1}]^-$ and $[\mathbf{3}]^-$ are closed-shell spin singlet configurations, whereas the ground states of $[\mathbf{2}]^-$ and $[\mathbf{4}]^-$ are spin triplets because of the two unpaired electrons of the U^{4+} ion. As shown previously by wavefunction calculations,[62,63] the ground state for Th(IV) is not strongly multi-configurational, and can therefore be described by (single determinant) Kohn-Sham DFT calculations with approximate functionals. Further evidence for the lack of multi-configurational character in the present systems are the large HOMO and LUMO gaps calculated for $[\mathbf{1}]^-$ and $[\mathbf{3}]^-$, at 3.0 and 3.4 eV, respectively. In other words, there are no complications due to the presence of nearly degenerate frontier orbitals in the DFT calculations for these molecules. Natural localized molecular orbital (NLMO) analysis (Figure 4 and Table S1) confirms the Cl→An dative bonding from the close-contact chlorine atoms of the

C_6Cl_5 ligands that is evident from the crystal structures. The lone pair donation from these chlorines have on average 7/8/6/5% weight at the actinide center in [**1/2/3/4**]$^-$, respectively. Not surprisingly, however, the dative bonding from the chloride ligands in [**3**]$^-$ and [**4**]$^-$ is stronger, with an average of 12 and 14% weight, respectively, at the actinide.

The NLMO analysis further shows that the Th-C_{ipso} interactions in [**1**]$^-$ and [**3**]$^-$ are quite similar (Figure 4). This similarity is also indicated by averaged Th-C_{ipso} Wiberg bond orders of 0.47 for [**1**]$^-$ and 0.49 for [**3**]$^-$, respectively. The interactions between the *ipso*-carbon atoms and thorium can be viewed as two-center two-electron (2c-2e) σ-donation bonding from the negatively charged ligand, with the Th weight in the corresponding σ-bonding NLMOs ranging from 14 to 15%. Of these weights, the Th 5f contributions are 24% in [**1**]$^-$ and 22% in [**3**]$^-$. In comparison, the two uranium complexes, [**2**]$^-$ and [**4**]$^-$, feature stronger covalency in their U-C bonds, along with more pronounced participation of the 5f AOs. The U weights in the σ-bonding NLMOs range from 18% in [**2**]$^-$ to 21% in [**4**]$^-$, of which the 5f contributions are 36% and 30%, respectively. The increased covalency, compared to the Th complexes, is reflected in increased averaged U-C_{ipso} Wiberg bond orders of 0.56 in [**2**]$^-$ and 0.64 in [**4**]$^-$, respectively. Similar bonding trends are observed for both $[An(C_6H_5)_6]^{2-}$ (An = Th, U) and $[AnMe_6]^{2-}$ (An = Th, U).[4,10,22] For example, the An-C bonds in $[U(C_6H_5)_6]^{2-}$ feature both a greater degree of covalency (23% total metal character for U vs. 16% for Th) and 5f character (38% for U vs. 20% for Th) than its Th analogue.[22]

Various approximate density functionals (BP86, PBE, and PBE0) were used for calculating the ^{13}C NMR chemical shifts for the *ipso*-carbon in [**1**]$^-$ and [**3**]$^-$. As seen in Table 2, the averaged calculated chemical shifts for both complexes are only weakly dependent on the choice of the functional. The calculated chemical shifts are in acceptable agreement with the measurements. We focus on the PBE/SO-PBE results in the following discussion, unless stated otherwise. For [**1**]$^-$,

the calculated C_{ipso} chemical shift is 203 ppm (expt. = 199 ppm), including a 27 ppm deshielding due to SO coupling. The C_{ipso} chemical shift in [**3**]$^-$ is calculated to be a bit larger than that in [**1**]$^-$, in agreement with the experiments, although the shift difference is slightly exaggerated in the calculations. The deshielding caused by SO coupling effects (ca. 29 ppm) is comparable that found in [**1**]$^-$, which reflects the similarity in their chemical bonding. The *ipso*-carbon SO deshielding in both [**1**]$^-$ and [**3**]$^-$ is correlated to the Th 5f and 6d character of the σ(Th-C) NLMO, and the overall weights of actinide AOs in these bonds (i.e., the degree of covalency). Our previous calculation[25] for $[Li(Et_2O)_2(THF)][UO_2(C_6Cl_5)_3]$ found a significantly larger SO deshielding, up to 68 ppm, due to a combination of large U weight (20% overall) and 5f contribution (43% of the U weight). This difference reflects both the change in element and the higher oxidation state in the uranyl example. Similarly, we would expect stronger SO effects for the *ipso*-carbon chemical shifts in our U(IV) complexes, compared to their thorium counterparts. However, the paramagnetism of [**2**]$^-$ and [**4**]$^-$ causes too much broadening of the relevant NMR signals for them to be observed. It also renders calculations of the NMR chemical shifts much more difficult,[64] and the role of SO coupling would not be as clear-cut as it is in the diamagnetic counterparts. Thus, we decided to forego calculations of the shifts for [**2**]$^-$ and [**4**]$^-$, because the bond analyses already paint a clear picture. Interestingly, the SO-induced chemical shift in $[Th(C_6H_5)_6]^{2-}$ (40 ppm, present work) is calculated to be 13 ppm larger than that of [**1**]$^-$ (27 ppm), despite the former complex having a smaller 5f weight in the Th contributions to the Th-C bonds. This decrease, however, is more than compensated for by the slightly greater overall Th weight and carbon 2s character in its Th-C bonds (Table 2 and Table S1).

Table 2. Calculated carbon shielding (σ) and chemical shift (δ) for the C_{ipso} atom center of [**1**]$^-$, [**3**]$^-$, and $[Th(C_6H_5)_6]^{2-}$, using various functionals.[a]

Complex	Functional	σ_{calc} (ppm)	δ_{calc} (ppm)	δ_{expt} (ppm)
TMS	BP86/SO-BP86	186.9 / 187.8	-	-
	PBE/SO-PBE	187.5 / 188.4	-	
	PBE0/SO-PBE0 (25%)[b]	192.2 / 193.0	-	
	PBE0/SO-PBE0 (40%)[b]	194.7 / 195.6	-	
[**1**]$^-$	BP86/SO-BP86	10.7 / –16.8	176.2 / 204.6	198.78
	PBE/SO-PBE	11.3 / –14.8	176.2 / 203.2	
	PBE0/SO-PBE0 (25%)	13.9 / –10.8	178.3 / 203.8	
	PBE0/SO-PBE0 (40%)	15.8 / –8.3	178.9 / 203.9	
[**3**]$^-$	BP86/SO-BP86	3.9 / –25.3	183.0 / 213.1	201.01
	PBE/SO-PBE	4.5 / –23.3	183.0 / 211.7	
	PBE0/SO-PBE0 (25%)	5.5 / –20.8	186.7 / 213.8	
	PBE0/SO-PBE0 (40%)	6.8 / –19.0	187.9 / 214.6	
$[Th(C_6H_5)_6]^{2-}$ [c]	PBE/SO-PBE	–21.2 /–60.1	208.7 / 248.5	220.5
	PBE0/SO-PBE0 (40%)	–15.5 / –53.4	210.2 / 249.0	

[a] NMR shifts calculated at the SO ZORA- level using the TZ2P basis set, with 'FXC' option. The calculated chemical shifts were averaged over equivalent C_{ipso} nuclei. Dichloromethane (solvent) was considered in the COSMO model for all the computations.

[b] The percentages in parentheses of functional column indicate the portion of exact exchange in the functional.

[c] For comparison, the carbon shielding and chemical shift for the C_{ipso} atom in C_3-symmetric $[Th(C_6H_5)_6]^{2-}$ was re-calculated using the same procedure as other complexes, such as using the 'FXC' option and same solvent (see computational details). The experimental chemical shift for this complex was taken from Ref. [19].

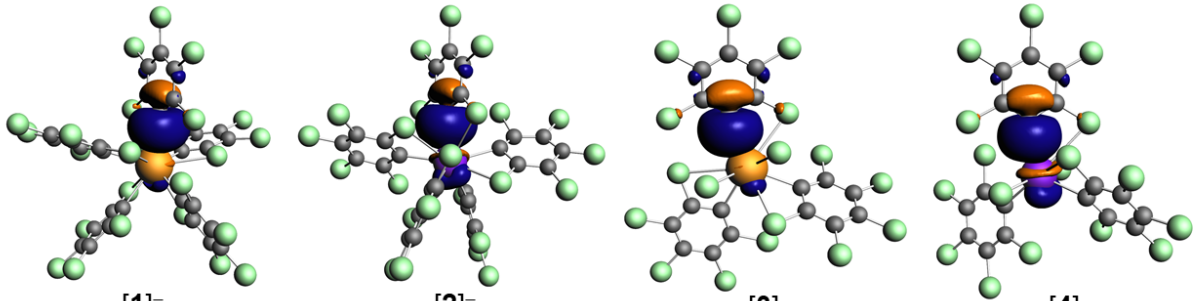

[**1**]$^-$
%Th(tot): 14
%Th(6d): 65
%Th(5f): 24

[**2**]$^-$
%U(tot): 18
%U(6d): 56
%U(5f): 36

[**3**]$^-$
%Th(tot): 15
%Th(6d): 65
%Th(5f): 22

[**4**]$^-$
%U(tot): 21
%U(6d): 58
%U(5f): 30

Figure 4. Representative An-C bonding NLMOs (An=Th or U) in [**1**]$^{-}$, [**2**]$^{-}$, [**3**]$^{-}$, and [**4**]$^{-}$. Weight-% metal character and 6d vs. 5f contributions at the metal averaged over equivalent NLMOs. (Isosurface values ±0.03 a.u. Color code for atoms: Th orange, U purple, Cl green, C gray.)

Conclusion

In summary, we have prepared and characterized two homoleptic actinide-aryl "ate" complexes, $[Li(DME)_2(Et_2O)]_2[Li(DME)_2][Th(C_6Cl_5)_5]_3$ and $[Li(Et_2O)_4][U(C_6Cl_5)_5]$, and have confirmed their formulation by X-ray crystallography. These two complexes represent the first isolated homoleptic perhaloaryl complexes of the actinides. They exhibit remarkable thermal stability – much greater than past homoleptic actinide aryl complexes – likely on account of the *o*-chloro substitution of the $[C_6Cl_5]^{-}$ ligand, combined with the many Cl→An dative interactions. Additionally, we prepared and characterized two heteroleptic actinide-aryl "ate" complexes, $[Li(DME)_2(Et_2O)][Li(Et_2O)_2][ThCl_3(C_6Cl_5)_3]$ and $[Li(Et_2O)_3][UCl_2(C_6Cl_5)_3]$. Analysis of the An-C bonding with these complexes by DFT reveals both greater covalency and greater 5f orbital participation in the U(IV) derivatives, consistent with past periodic trends. In addition, a DFT analysis of the C_{ipso} chemical shifts in the two Th complexes reveals modest levels of spin-orbit induced shielding due to 5f participation in the Th-C bonds, providing us with an opportunity to further refine the ^{13}C NMR spectroscopic analysis of An-L bonding.

ASSOCIATED CONTENT

Supporting Information. Experimental procedures, crystallographic details (as CIF files), computational results, and spectral data for complexes [Li][**1**]-[Li][**4**]. See DOI:

AUTHOR INFORMATION

Corresponding Author

hayton@chem.ucsb.edu, jochena@buffalo.edu

ACKNOWLEDGEMENTS

This work was supported by the U.S. Department of Energy, Office of Basic Energy Sciences, Chemical Sciences, Biosciences, and Geosciences Division under Contract DE-SC-0001861. This research made use of the 400 MHz NMR Spectrometer in the Department of Chemistry, an NIH SIG (1S10OD012077-01A1), and a 500 MHz NMR Spectrometer supported by an NSF Major Research Instrumentation (MRI) Award 1920299. J.A. acknowledges support for the theoretical component of this study by the U.S. Department of Energy, Office of Science, Heavy Element Chemistry program, grant DE-SC0001136. We thank the Center for Computational Research (CCR) at the University of Buffalo for providing computational resources.

References

(1) Jones, M. B.; Gaunt, A. J. Recent Developments in Synthesis and Structural Chemistry of Nonaqueous Actinide Complexes. *Chem. Rev.* **2013**, *113*, 1137–1198.

(2) Liddle, S. T. The Renaissance of Non-Aqueous Uranium Chemistry. *Angew. Chem. Int. Ed.* **2015**, *54*, 8604–8641.

(3) A. Johnson, S.; C. Bart, S. Achievements in Uranium Alkyl Chemistry: Celebrating Sixty Years of Synthetic Pursuits. *Dalton Trans.* **2015**, *44*, 7710–7726.

(4) Sears, J. D.; Sergentu, D.-C.; Baker, T. M.; Brennessel, W. W.; Autschbach, J.; Neidig, M. L. The Exceptional Diversity of Homoleptic Uranium–Methyl Complexes. *Angew. Chem.* **2020**, *132*, 13688–13692.

(5) Van der Sluys, W. G.; Burns, C. J.; Sattelberger, A. P. First Example of a Neutral Homoleptic Uranium Alkyl. Synthesis, Properties, and Structure of $U[CH(SiMe_3)_2]_3$. *Organometallics* **1989**, *8*, 855–857.

(6) Kraft, S. J.; Fanwick, P. E.; Bart, S. C. Carbon–Carbon Reductive Elimination from Homoleptic Uranium(IV) Alkyls Induced by Redox-Active Ligands. *J. Am. Chem. Soc.* **2012**, *134*, 6160–6168.

(7) Johnson, S. A.; Kiernicki, J. J.; Fanwick, P. E.; Bart, S. C. New Benzylpotassium Reagents and Their Utility for the Synthesis of Homoleptic Uranium(IV) Benzyl Derivatives. *Organometallics* **2015**, *34*, 2889–2895.

(8) Fortier, S.; Melot, B. C.; Wu, G.; Hayton, T. W. Homoleptic Uranium(IV) Alkyl Complexes: Synthesis and Characterization. *J. Am. Chem. Soc.* **2009**, *131*, 15512–15521.

(9) Fortier, S.; Walensky, J. R.; Wu, G.; Hayton, T. W. High-Valent Uranium Alkyls: Evidence for the Formation of $U^{VI}(CH_2SiMe_3)_6$. *J. Am. Chem. Soc.* **2011**, *133*, 11732–11743.

(10) Seaman, L. A.; Walensky, J. R.; Wu, G.; Hayton, T. W. In Pursuit of Homoleptic Actinide Alkyl Complexes. *Inorg. Chem.* **2013**, *52*, 3556–3564.

(11) Lauke, H.; Swepston, P. J.; Marks, T. J. Synthesis and Characterization of a Homoleptic Actinide Alkyl. The Heptamethylthorate(IV) Ion: A Complex with Seven Metal-Carbon .Sigma. Bonds. *J. Am. Chem. Soc.* **1984**, *106*, 6841–6843.

(12) Cruz, C. A.; Emslie, D. J. H.; Harrington, L. E.; Britten, J. F.; Robertson, C. M. Extremely Stable Thorium(IV) Dialkyl Complexes Supported by Rigid Tridentate 4,5-Bis(Anilido)Xanthene and 2,6-Bis(Anilidomethyl)Pyridine Ligands. *Organometallics* **2007**, *26*, 692–701.

(13) C. Behrle, A.; J. Myers, A.; Rungthanaphatsophon, P.; W. Lukens, W.; L. Barnes, C.; R. Walensky, J. Uranium(III) and Thorium(IV) Alkyl Complexes as Potential Starting Materials. *Chem. Commun.* **2016**, *52*, 14373–14375.

(14) Myers, A. J.; Tarlton, M. L.; Kelley, S. P.; Lukens, W. W.; Walensky, J. R. Synthesis and Utility of Neptunium(III) Hydrocarbyl Complex. *Angew. Chem. Int. Ed.* **2019**, *58*, 14891–14895.

(15) Kraft, S. J.; Fanwick, P. E.; Bart, S. C. Exploring the Insertion Chemistry of Tetrabenzyluranium Using Carbonyls and Organoazides. *Organometallics* **2013**, *32*, 3279–3285.

(16) Matson, E. M.; Franke, S. M.; Anderson, N. H.; Cook, T. D.; Fanwick, P. E.; Bart, S. C. Radical Reductive Elimination from Tetrabenzyluranium Mediated by an Iminoquinone Ligand. *Organometallics* **2014**, *33*, 1964–1971.

(17) Duhović, S.; Khan, S.; L. Diaconescu, P. In Situ Generation of Uranium Alkyl Complexes. *Chem. Commun.* **2010**, *46*, 3390–3392.

(18) Johnson, S. A.; Higgins, R. F.; Abu-Omar, M. M.; Shores, M. P.; Bart, S. C. Mechanistic Insights into Concerted C–C Reductive Elimination from Homoleptic Uranium Alkyls. *Organometallics* **2017**, *36*, 3491–3497.

(19) Pedrick, E. A.; Hrobárik, P.; Seaman, L. A.; Wu, G.; Hayton, T. W. Synthesis, Structure and Bonding of Hexaphenyl Thorium(IV): Observation of a Non-Octahedral Structure. *Chem. Commun.* **2016**, *52*, 689–692.
(20) Boreen, M. A.; Parker, B. F.; Lohrey, T. D.; Arnold, J. A Homoleptic Uranium(III) Tris(Aryl) Complex. *J. Am. Chem. Soc.* **2016**, *138*, 15865–15868.
(21) Seaman, L. A.; Pedrick, E. A.; Tsuchiya, T.; Wu, G.; Jakubikova, E.; Hayton, T. W. Comparison of the Reactivity of 2-Li-$C_6H_4CH_2NMe_2$ with MCl_4 (M=Th, U): Isolation of a Thorium Aryl Complex or a Uranium Benzyne Complex. *Angew. Chem. Int. Ed.* **2013**, *52*, 10589–10592.
(22) Wolford, N. J.; Sergentu, D.-C.; Brennessel, W. W.; Autschbach, J.; Neidig, M. L. Homoleptic Aryl Complexes of Uranium (IV). *Angew. Chem. Int. Ed.* **2019**, *58*, 10266–10270.
(23) Graves, C. R.; Schelter, E. J.; Cantat, T.; Scott, B. L.; Kiplinger, J. L. A Mild Protocol To Generate Uranium(IV) Mixed-Ligand Metallocene Complexes Using Copper(I) Iodide. *Organometallics* **2008**, *27*, 5371–5378.
(24) Evans, W. J.; Miller, K. A.; Ziller, J. W.; DiPasquale, A. G.; Heroux, K. J.; Rheingold, A. L. Formation of $(C_5Me_5)_2U(EPh)Me$, $(C_5Me_5)_2U(EPh)_2$, and $(C_5Me_5)_2U(H_2\text{-}TeC_6H_4)$ from $(C_5Me_5)_2UMe_2$ and PhEEPh (E = S, Se, Te). *Organometallics* **2007**, *26*, 4287–4293.
(25) Ordoñez, O.; Yu, X.; Wu, G.; Autschbach, J.; Hayton, T. W. Synthesis and Characterization of Two Uranyl-Aryl "Ate" Complexes. *Chem. Eur. J.* **2021**, *27*, 5885–5889.
(26) Mullane, K. C.; Hrobárik, P.; Cheisson, T.; Manor, B. C.; Carroll, P. J.; Schelter, E. J. ^{13}C NMR Shifts as an Indicator of U–C Bond Covalency in Uranium(VI) Acetylide Complexes: An Experimental and Computational Study. *Inorg. Chem.* **2019**, *58*, 4152–4163.
(27) Smiles, D. E.; Wu, G.; Hrobárik, P.; Hayton, T. W. Synthesis, Thermochemistry, Bonding, and ^{13}C NMR Chemical Shift Analysis of a Phosphorano-Stabilized Carbene of Thorium. *Organometallics* **2017**, *36*, 4519–4524.
(28) Seaman, L. A.; Hrobárik, P.; Schettini, M. F.; Fortier, S.; Kaupp, M.; Hayton, T. W. A Rare Uranyl(VI)–Alkyl Ate Complex $[Li(DME)_{1.5}]_2[UO_2(CH_2SiMe_3)_4]$ and Its Comparison with a Homoleptic Uranium(VI)–Hexaalkyl. *Angew. Chem. Int. Ed.* **2013**, *52*, 3259–3263.
(29) Staun, S. L.; Sergentu, D.-C.; Wu, G.; Autschbach, J.; Hayton, T. W. Use of ^{15}N NMR Spectroscopy to Probe Covalency in a Thorium Nitride. *Chem. Sci.* **2019**, *10*, 6431–6436.
(30) Smiles, D. E.; Wu, G.; Hrobárik, P.; Hayton, T. W. Use of ^{77}Se and ^{125}Te NMR Spectroscopy to Probe Covalency of the Actinide-Chalcogen Bonding in $[Th(E_n)\{N(SiMe_3)_2\}_3]^-$ (E = Se, Te; *n* = 1, 2) and Their Oxo-Uranium(VI) Congeners. *J. Am. Chem. Soc.* **2016**, *138*, 814–825.
(31) Wu, W.; Rehe, D.; Hrobárik, P.; Kornienko, A. Y.; Emge, T. J.; Brennan, J. G. Molecular Thorium Compounds with Dichalcogenide Ligands: Synthesis, Structure, ^{77}Se NMR Study, and Thermolysis. *Inorg. Chem.* **2018**, *57*, 14821–14833.
(32) Hrobárik, P.; Hrobáriková, V.; Greif, A. H.; Kaupp, M. Giant Spin-Orbit Effects on NMR Shifts in Diamagnetic Actinide Complexes: Guiding the Search of Uranium(VI) Hydride Complexes in the Correct Spectral Range. *Angew. Chem. Int. Ed.* **2012**, *51*, 10884–10888.
(33) Panetti, G. B.; Sergentu, D.-C.; Gau, M. R.; Carroll, P. J.; Autschbach, J.; Walsh, P. J.; Schelter, E. J. Isolation and Characterization of a Covalent Ce^{IV}-Aryl Complex with an Anomalous ^{13}C Chemical Shift. *Nat. Commun.* **2021**, *12*, 1713.
(34) Vícha, J.; Novotný, J.; Komorovsky, S.; Straka, M.; Kaupp, M.; Marek, R. Relativistic Heavy-Neighbor-Atom Effects on NMR Shifts: Concepts and Trends Across the Periodic Table. *Chem. Rev.* **2020**, *120*, 7065–7103.
(35) García-Monforte, M. A.; Alonso, P. J.; Forniés, J.; Menjón, B. New Advances in Homoleptic Organotransition-Metal Compounds: The Case of Perhalophenyl Ligands. *Dalton Trans.* **2007**, *31*, 3347–3359.

(36) Alonso, P. J.; Forniés, J.; García-Monforte, M. A.; Martín, A.; Menjón, B. New Homoleptic Organometallic Derivatives of Vanadium(III) and Vanadium(IV): Synthesis, Characterization, and Study of Their Electrochemical Behaviour. *Chem. Eur. J.* **2005**, *11*, 4713–4724.
(37) Alonso, P. J.; Arauzo, A. B.; Forniés, J.; García-Monforte, M. A.; Martín, A.; Martínez, J. I.; Menjón, B.; Rillo, C.; Sáiz-Garitaonandia, J. J. A Square-Planar Organoiron(III) Compound with a Spin-Admixed State. *Angew. Chem. Int. Ed.* **2006**, *45*, 6707–6711.
(38) Alonso, P. J.; Forniés, J.; García-Monforte, M. A.; Martín, A.; Menjón, B.; Rillo, C. A New Series of Homoleptic, Paramagnetic Organochromium Derivatives: Synthesis, Characterization, and Study of Their Magnetic Properties. *Chem. Eur. J.* **2002**, *8*, 4056–4065.
(39) Alonso, P. J.; Falvello, L. R.; Forniés, J. Synthesis and First Structural Characterisation of a Homoleptic Tetraorganochromate(III) Salt. *Chem. Commun.* **1998**, *16*, 1721–1722.
(40) Alonso, P. J.; Forniés, J.; García-Monforte, M. A.; Martín, A.; Menjón, B. The First Structurally Characterised Homolepticorganovanadium(III) Compound. *Chem. Commun.* **2001**, *20*, 2138–2139.
(41) Garcia, M. P.; Jimenez, M. V.; Oro, L. A.; Lahoz, F. J.; Tiripicchio, M. C.; Tiripicchio, A. A Homoleptic Mononuclear Iridium(II) Organometallic Complex: Synthesis and x-Ray Structure of $[Ir(C_6Cl_5)_4]^{2-}$. *Organometallics* **1993**, *12*, 4660–4663.
(42) García, M. P.; Jiménez, M. V.; Lahoz, F. J.; López, J. A.; Oro, L. A. Synthesis of the Homoleptic Rhodium(III) Complex $[Rh(C_6Cl_5)_3]$. Molecular Structures of $[Rh(C_6Cl_5)_3]$ and $[Rh(C_6Cl_4–C_6Cl_4)(C_6Cl_5)(SC_4H_8)_2]$. *J. Chem. Soc., Dalton Trans.* **1998**, *24*, 4211–4214.
(43) Fornies, J.; Menjon, B.; Sanz-Carrillo, R. M.; Tomas, M.; Connelly, N. G.; Crossley, J. G.; Orpen, A. G. Synthesis and Structural Characterization of the First Isolated Homoleptic Organoplatinum(IV) Compound: $[Pt(C_6Cl_5)_4]$. *J. Am. Chem. Soc.* **1995**, *117*, 4295–4304.
(44) Ara, I.; Forniés, J.; García-Monforte, M. A.; Martín, A.; Menjón, B. Synthesis and Characterization of Pentachlorophenyl–Metal Derivatives with D^0 and D^{10} Electron Configurations. *Chem. Eur. J.* **2004**, *10*, 4186–4197.
(45) Rausch, M. D.; Tibbetts, F. E.; Gordon, H. B. Perhaloaryl-Metal Chemistry: II. Pentachlorophenyllithium. *J. Organomet. Chem.* **1966**, *5*, 493–500.
(46) Fagan, P. J.; Manriquez, J. M.; Maatta, E. A.; Seyam, A. M.; Marks, T. J. Synthesis and Properties of Bis(Pentamethylcyclopentadienyl) Actinide Hydrocarbyls and Hydrides. A New Class of Highly Reactive f-Element Organometallic Compounds. *J. Am. Chem. Soc.* **1981**, *103*, 6650–6667.
(47) Cirera, J.; Ruiz, E.; Alvarez, S. Continuous Shape Measures as a Stereochemical Tool in Organometallic Chemistry. *Organometallics* **2005**, *24*, 1556–1562.
(48) Ruiz-Martínez, A.; Alvarez, S. Stereochemistry of Compounds with Coordination Number Ten. *Chem. Eur. J.* **2009**, *15*, 7470–7480.
(49) Ruiz-Martínez, A.; Casanova, D.; Alvarez, S. Polyhedral Structures with an Odd Number of Vertices: Nine-Atom Clusters and Supramolecular Architectures. *Dalton Trans.* **2008**, *19*, 2583–2591.
(50) Ruiz-Martínez, A.; Casanova, D.; Alvarez, S. Polyhedral Structures with an Odd Number of Vertices: Nine-Coordinate Metal Compounds. *Chem. Eur. J.* **2008**, *14*, 1291–1303.
(51) Pedrick, E. A.; Wu, G.; Kaltsoyannis, N.; Hayton, T. W. Reductive Silylation of a Uranyl Dibenzoylmethanate Complex: An Example of Controlled Uranyl Oxo Ligand Cleavage. *Chem. Sci.* **2014**, *5*, 3204–3213.
(52) Schnaars, D. D.; Wu, G.; Hayton, T. W. Reduction of Pentavalent Uranyl to U(IV) Facilitated by Oxo Functionalization. *J. Am. Chem. Soc.* **2009**, *131*, 17532–17533.
(53) Yin, H.; J. Lewis, A.; J. Williams, U.; J. Carroll, P.; J. Schelter, E. Fluorinated Diarylamide Complexes of Uranium(III, IV) Incorporating Ancillary Fluorine-to-Uranium Dative Interactions. *Chem. Sci.* **2013**, *4*, 798–805.

(54) Shannon, R. D. Revised Effective Ionic Radii and Systematic Studies of Interatomic Distances in Halides and Chalcogenides. *Acta Cryst A* **1976**, *32*, 751–767.
(55) Zabrodsky, H.; Peleg, S.; Avnir, D. Continuous Symmetry Measures. *J. Am. Chem. Soc.* **1992**, *114*, 7843–7851.
(56) Cantat, T.; Scott, B. L.; Kiplinger, J. L. Convenient Access to the Anhydrous Thorium Tetrachloride Complexes $ThCl_4(DME)_2$, $ThCl_4$(1,4-Dioxane)$_2$ and $ThCl_4(THF)_{3.5}$ Using Commercially Available and Inexpensive Starting Materials. *Chem. Commun.* **2010**, *46*, 919–921.
(57) Schnaars, D. D.; Wu, G.; Hayton, T. W. Reactivity of UH_3 with Mild Oxidants. *Dalton Trans.* **2008**, *44*, 6121–6126.
(58) Pedrick, E. A.; Seaman, L. A.; Scott, J. C.; Griego, L.; Wu, G.; Hayton, T. W. Synthesis and Reactivity of a U(IV) Dibenzyne Complex. *Organometallics* **2016**, *35*, 494–502.
(59) Glendening, E. D.; Landis, C. R.; Weinhold, F. NBO 6.0: Natural Bond Orbital Analysis Program. *J. Comput. Chem.* **2013**, *34*, 1429–1437.
(60) Autschbach, J. The Role of the Exchange-Correlation Response Kernel and Scaling Corrections in Relativistic Density Functional Nuclear Magnetic Shielding Calculations with the Zeroth-Order Regular Approximation. *Mol. Phys.* **2013**, *111*, 2544–2554.
(61) E. J. Baerends*, T. Ziegler, A. J. Atkins, J. Autschbach, O. Baseggio, D. Bashford, A. Bérces, F. M. Bickelhaupt, C. Bo, P. M. Boerrigter, L. Cavallo, C. Daul, D. P. Chong, D. V. Chulhai, L. Deng, R. M. Dickson, J. M. Dieterich, D. E. Ellis, M. v. Faassen, L. Fan, T. H. Fischer, C. F. Guerra, M. Franchini, A. Ghysels, A. Giammona, S. J. A. v. Gisbergen, A. Goez,; A. W. Götz, J. A. Groeneveld, O. V. Gritsenko, M. Grüning, S. Gusarov, F. E. Harris, P. v. d. Hoek, Z. Hu, C. R. Jacob, H. Jacobsen, L. Jensen, L. Joubert, J. W. Kaminski, G. v. Kessel, C. König, F. Kootstra, A. Kovalenko, M. V. Krykunov, E. v. Lenthe, D. A. McCormack, A. Michalak, M. Mitoraj, S. M. Morton, J. Neugebauer, V. P. Nicu, L. Noodleman, V. P. Osinga, S. Patchkovskii, M. Pavanello, C. A. Peeples, P. H. T. Philipsen, D. Post, C. C. Pye, H. Ramanantoanina, P. Ramos, W. Ravenek, J. I. Rodríguez, P. Ros, R. Rüger, P. R. T. Schipper, D. Schlüns, H. v. Schoot, G. Schreckenbach, J. S. Seldenthuis, M. Seth, J. G. Snijders, M. Solà, M. Stener, M. Swart, D. Swerhone, V. Tognetti, G. t. Velde, P. Vernooijs, L. Versluis, L. Visscher, O. Visser, F. Wang, T. A. Wesolowski, E. M. v. Wezenbeek, G. Wiesenekker, S. K. Wolff, T. K. Woo, A. L. Yakovlev,* Amsterdam Density Functional. 2017 Ed.; SCM, Theoretical Chemistry, Vrije Universiteit Amsterdam, The Netherlands, **2017**. https://www.scm.com.
(62) Assefa, M.; Sergentu, D.-C.; Seaman, L.; Wu, G.; Autschbach, J.; Hayton, T. Synthesis, Characterization, and Electrochemistry of the Homoleptic f Element Ketimide Complexes, $[Li]_2[M(N{=}CtBuPh)_6]$ (M = Ce, Th), *Inorg. Chem.* **2019**, *58*, 12654–12661.
(63) Ganguly, G.; Sergentu, D.-C.; Autschbach, J. Ab Initio Analysis of Metal-Ligand Bonding in $An(COT)_2$, An = Th, U, in Their Ground- and Core-Excited States, *Chem. Eur. J.* **2020**, *26*, 1776–1788.
(64) Autschbach, J. Chapter One - NMR Calculations for Paramagnetic Molecules and Metal Complexes. *Annu. Rep. Comput. Chem.*; Dixon, D. A., Ed.; Elsevier, 2015; Vol. 11, pp 3–36.

Entry for the Table of Contents

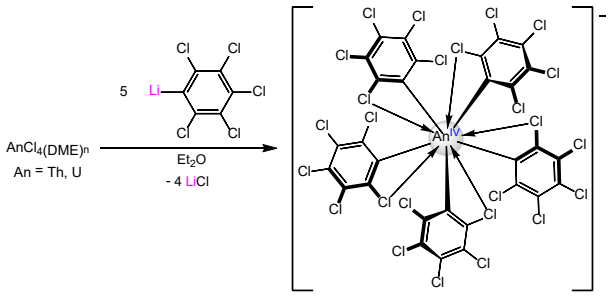

The homoleptic actinide-aryl "ate" complexes, $[Li(DME)_2(Et_2O)]_2[Li(DME)_2][Th(C_6Cl_5)_5]_3$ and $[Li(Et_2O)_4][U(C_6Cl_5)_5]$, exhibit appreciable thermal stability, on account of the *o*-chloro substitution within the $[C_6Cl_5]^-$ ligand, combined with the many Cl→An dative interactions.